The Astrophysical Journal, 809:109 (8pp), 2015 August 20 doi:10.1088/0004-637X/809/2/109

BROAD BALMER WINGS IN BA HYPER/SUPERGIANTS DISTORTED BY DIFFUSE INTERSTELLAR BANDS: FIVE EXAMPLES IN THE 30 DORADUS REGION FROM THE VLT-FLAMES TARANTULA SURVEY

Nolan R. Walborn[1], Hugues Sana[1], Christopher J. Evans[2], William D. Taylor[2], Elena Sabbi[1], Rodolfo H. Barbá[3], Nidia I. Morrell[4], Jesús Maíz Apellániz[5], Alfredo Sota[6], Philip L. Dufton[7], Catherine M. McEvoy[7], J. Simon Clark[8], Nevena Markova[9], and Krzysztof Ulaczyk[10]

[1] Space Telescope Science Institute, 3700 San Martin Drive, Baltimore, MD 21218, USA; walborn@stsci.edu, hsana@stsci.edu, sabbi@stsci.edu
[2] UK Astronomy Technology Centre, Royal Observatory Edinburgh, Blackford Hill, Edinburgh EH9 3HJ, UK; chris.evans@stfc.ac.uk, william.taylor@stfc.ac.uk
[3] Departamento de Física y Astronomía, Universidad de La Serena, Cisternas 1200 Norte, La Serena, Chile; rbarba@dfuls.cl
[4] Las Campanas Observatory, Carnegie Observatories, Casilla 601, La Serena, Chile; nmorrell@lco.cl
[5] Centro de Astrobiología, CSIC-INTA, Campus ESAC, Apartado Postal 78, E-28691 Villanueva de la Cañada, Madrid, Spain; jmaiz@cab.inta-csic.es
[6] Instituto de Astrofísica de Andalucía—CSIC, Glorieta de la Astronomía s/n, E-18008 Granada, Spain; sota@iaa.es
[7] Astrophysics Research Centre, School of Mathematics and Physics, Queen's University Belfast, Belfast BT7 1NN, UK; p.dufton@qub.ac.uk, cmcevoy14@qub.ac.uk
[8] Department of Physics and Astronomy, The Open University, Milton Keynes MK7 6AA, UK; jsc@star.ucl.ac.uk
[9] Institute of Astronomy, National Astronomical Observatory, Bulgarian Academy of Sciences, P.O. Box 136, 4700 Smoljan, Bulgaria; nmarkova@astro.bas.bg
[10] Warsaw University Observatory, Al. Ujazdowskie 4, 00-478 Warsaw, Poland; kulaczyk@astrouw.edu.pl
Received 2014 December 11; accepted 2015 July 11; published 2015 August 14

ABSTRACT

Extremely broad emission wings at Hβ and Hα have been found in VLT-FLAMES Tarantula Survey data for five very luminous BA supergiants in or near 30 Doradus in the Large Magellanic Cloud. The profiles of both lines are extremely asymmetrical, which we have found to be caused by very broad diffuse interstellar bands (DIBs) in the longward wing of Hβ and the shortward wing of Hα. These DIBs are well known to interstellar but not to many stellar specialists, so that the asymmetries may be mistaken for intrinsic features. The broad emission wings are generally ascribed to electron scattering, although we note difficulties for that interpretation in some objects. Such profiles are known in some Galactic hyper/supergiants and are also seen in both active and quiescent Luminous Blue Variables (LBVs). No prior or current LBV activity is known in these 30 Dor stars, although a generic relationship to LBVs is not excluded; subject to further observational and theoretical investigation, it is possible that these very luminous supergiants are approaching the LBV stage for the first time. Their locations in the HRD and presumed evolutionary tracks are consistent with that possibility. The available evidence for spectroscopic variations of these objects is reviewed, while recent photometric monitoring does not reveal variability. A search for circumstellar nebulae has been conducted, with an indeterminate result for one of them.

Key words: Magellanic Clouds – stars: early-type – stars: massive – stars: peculiar – stars: variables: S Doradus – supergiants

1. INTRODUCTION

A property of Luminous Blue Variables (LBVs) both in outburst and quiescense is the occurrence of extremely broad Balmer emission wings, usually ascribed to electron scattering in dense extended atmospheres or envelopes (Bernat & Lambert 1978; Hubeny & Leitherer 1989; Santolaya-Rey et al. 1997; Najarro & Hillier 2012). In some cases, a narrow P Cygni profile is superimposed, producing the "Prussian Helmet" morphology. Examples may be found in Stahl et al. (1985), Hutsemékers & van Drom (1991), and Walborn & Fitzpatrick (2000). Similar profiles are observed in some very luminous Galactic B supergiants with no evidence of previous LBV activity (e.g., Lennon et al. 1992; Marco & Negueruela 2009; Clark et al. 2012), although it would not be surprising if these objects were approaching the LBV stage. A puzzling property of the Hβ wings is their apparent asymmetry, more extended and shallow shortward but curtailed and steeper longward. As emphasized by Hutsemékers and Van Drom, that morphology cannot be produced by electron scattering; moreover, it is not shared by Hα. Here we propose a likely resolution of this discrepancy.

We report the discovery of these broad Balmer wings in five BA hyper/supergiants in or near the 30 Doradus Nebula of the Large Magellanic Cloud (LMC), but again, with no record or known evidence of outbursts. The only confirmed LBV in the 30 Dor region is Radcliffe (R) 143 (Feast et al. 1960), located in an evolved association immediately SE of the main Tarantula Nebula (Walborn & Blades 1997). Feast et al. reported an F-supergiant spectrum, but Parker et al. (1993) discovered it two magnitudes fainter with a late-B spectrum (see also Walborn 1997), establishing its LBV nature. Smith et al. (1998; see also Weis 2003) subsequently found ejected nitrogen-rich circumstellar nebulosity, another frequent characteristic of LBVs and indicative of a larger, earlier eruption. The spectra, locations, and known variability of these five 30 Dor objects, one of which may be associated with R143, are discussed below, as well as a search for circumstellar nebulae.

2. OBSERVATIONS

The primary spectroscopic data used here are from the VLT-FLAMES Tarantula Survey (VFTS; ESO Large Programme 182.D-0222, PI CJE). Full details of the instrumental parameters and data reductions were provided by Evans et al. (2011, 2015 and references therein). In brief, the observations were obtained in the Medusa–Giraffe configuration of the Fibre

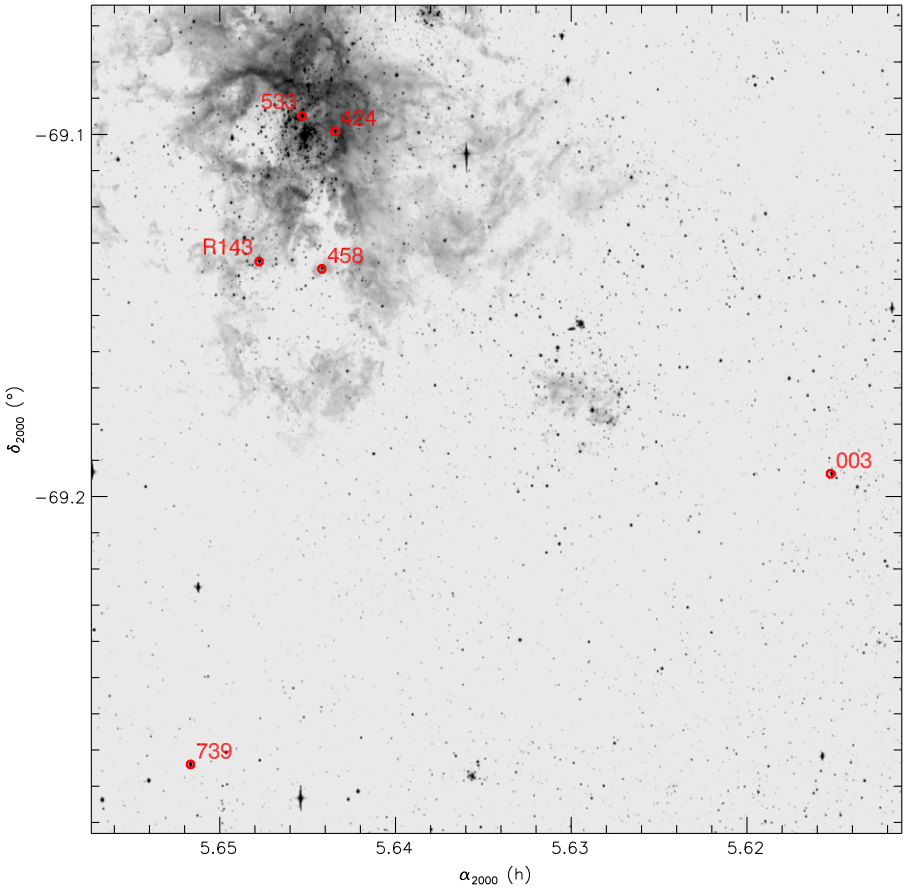

Figure 1. Locations of the five VFTS objects in the 30 Dor field. The known LBV R143 is also identified. The extended stellar object at upper left is the cluster core R136. The image is in the *V* band from the Wide Field Imager on the ESO/MPG 2.2 m telescope.

Large Array Multi-Element Spectrograph (FLAMES; Pasquini et al. 2002) at the Very Large Telescope (VLT) on Cerro Paranal, Chile. Each target was observed with the standard LR02 and LR03 settings of the Giraffe spectrograph, providing coverage of 3960–5071 Å at a spectral resolving power (R) of 7000–8500. At least six observations were obtained with the LR02 setting to support the investigation of spectroscopic binaries (Sana et al. 2013; Evans et al. 2015). In addition, the Hα region was observed with the HR15N setting at R of 16,000. Most of the observations were done during 2008 October through 2009 February, with a final epoch in 2009 October to extend the binary period sensitivity.

3. RESULTS

The locations of the five VFTS objects in the field of 30 Dor are shown in Figure 1, along with that of R143. Coordinates and photometry are provided by Evans et al. (2011). Their full blue-violet spectra are displayed in Figure 2, while enlargements of their Hβ and Hα profiles are shown in Figure 3. Several interesting common properties of these Balmer profiles are discussed here, while further details of the individual objects and spectra are considered in following subsections.

The similar, marked asymmetry of the broad Hβ wings in all the objects is remarkable and characteristic: the shortward wings are more extended and shallower, while the longward ones are shorter and steeper (Figure 3). The broad emission has a full width at zero intensity of ∼50 Å or 3000 km s^{-1}, far too large to be ascribed to a Doppler effect, which is why such profiles have been interpreted in terms of electron scattering. (Typical wind terminal velocities of Galactic B1–2 hypergiants are a few hundred km s^{-1}; Crowther et al. 2006; Clark et al. 2012.) In luminous late-B and -A supergiants with lower mass-loss rates, peculiar Balmer emission profiles can be produced by NLTE effects (Hubeny & Leitherer 1989; Santolaya-Rey et al. 1997; Puls et al. 1998). The observed peak intensities of the broad emission wings are 1%–3% relative to the continuum.

The Hα wings are entirely different from those of Hβ, with a broad absorption depression in the *shortward* one. Our first thought on the latter was a feature related to the stellar winds, although its similarity across the entire B-type spectral range (Figure 2) was disconcerting, as was its extent relative to the stellar-wind velocities of such objects. Subsequently, we realized that the depths of these features are correlated with the reddenings of the stars, immediately suggesting an origin related to extinction and consultation of Herbig (1995), who indeed lists a broad, shallow Diffuse Interstellar Band (DIB) centered at 6533 Å, with an FWHM of 21 Å, in good agreement with the data. An analogous origin of the Hβ asymmetry was then suggested by the extreme case of Cygnus OB2-12, as shown in Figure 4. Here the DIB responsible is centered at 4882 Å with an FWHM of 25 Å according to Herbig, but Maíz Apellániz et al. (2014) have decomposed it into two features, a narrower one centered at 4880 and a broader one at 4887 Å.

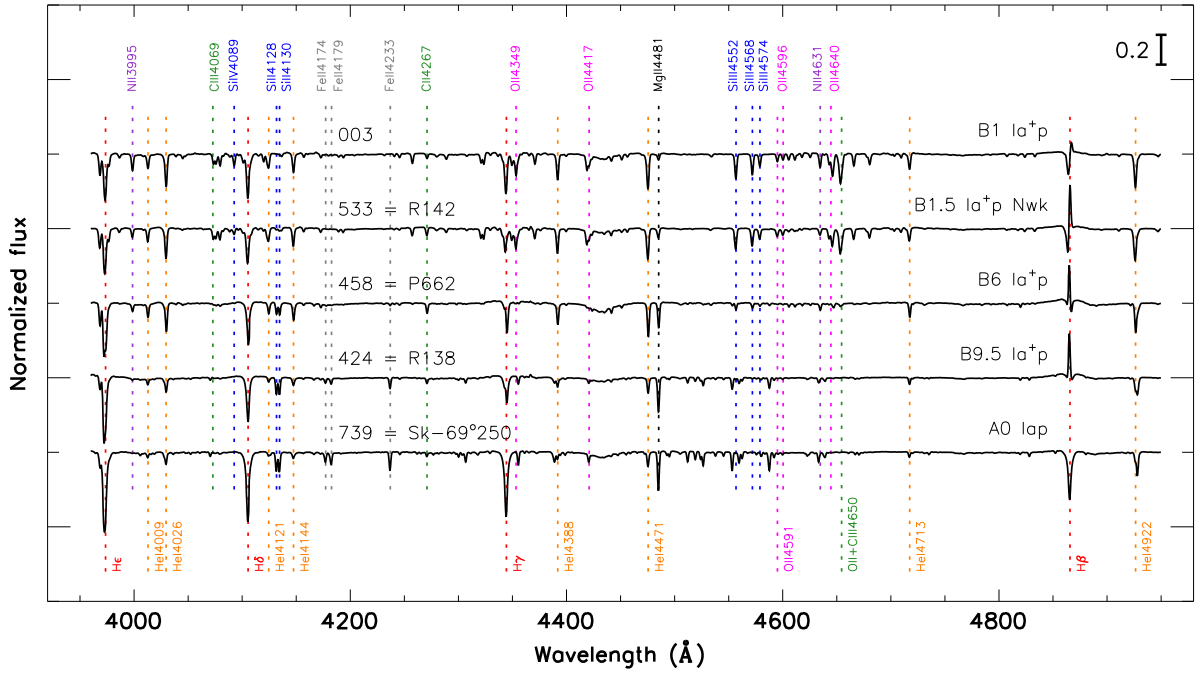

Figure 2. Full violet through green spectra of the five VFTS objects. Note the extreme differences between the CNO spectra of VFTS 003 and 533 despite their similar spectral types, as discussed in the text. Some features near those identified in the earlier-type spectra arise from different, lower-ionization species in the later types; e.g., O II λ4349 is replaced by Fe II λ4352. Enlargements of the Hβ profiles are shown in Figure 3.

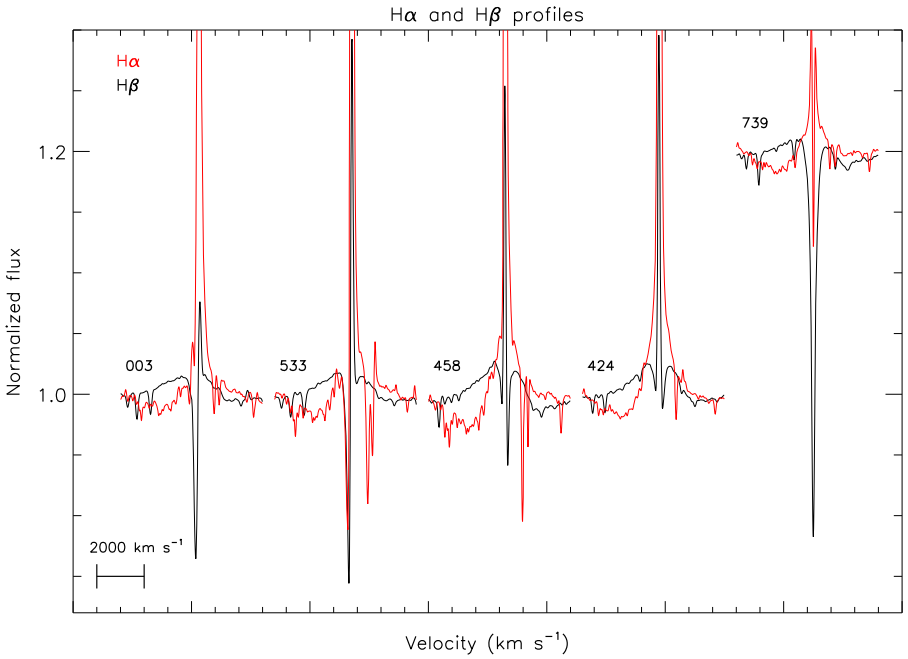

Figure 3. Enlargements of the Hβ profiles (black) to show the very similar, extensive asymmetrical wings in all of the spectra, with the corresponding Hα profiles (red) superimposed. The narrow Hβ emission in VFTS 533 is a blend of a stellar P Cygni profile and nebular emission, whereas in VFTS 003 it is dominated by the stellar profile, but in VFTS 458 and 424 it is entirely nebular. The apparent shortward, broad absorption troughs in the Hα profiles are actually the diffuse interstellar band (DIB) at 6533 Å (Herbig 1995; Walborn & Howarth 2000); E_{B-V} ranges from 0.30 to 0.68 for these objects, with the largest value corresponding to VFTS 458. The VFTS 739 profile has been shifted by +0.2 continuum unit for clarity.

3.1. VFTS 003 = HD 38029B

This luminous B supergiant is located only 2″.8 from and is most likely associated in a small cluster with the WC4+O6–6.5 III system HD 38029A = VFTS 002 (Evans et al. 2011), which is currently much fainter in the optical but likely also descends from a very massive progenitor. To our knowledge, VFTS 003 lacks accurate, spatially resolved optical photometry; in fact, there is confusion in the literature about the magnitudes of the two stars. Remarkably, Sanduleak (1970) resolved them and correctly gave their relative positions and magnitudes; in particular, he lists m_{pg} of 11.8 for the B supergiant and 14.2 for

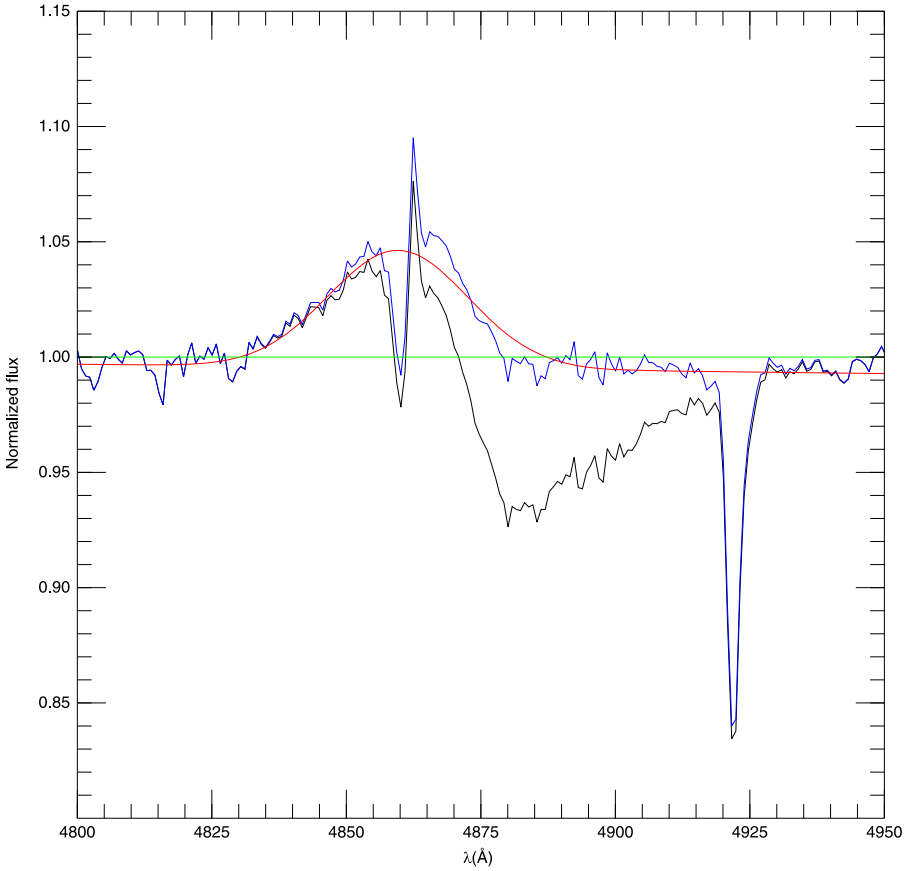

Figure 4. Region of Hβ in the spectrum of the extremely reddened star Cygnus OB2–12 ($E_{B-V} = 3.54$, or $E(4405-5495) = 3.79$; Maíz Apellániz 2013), as observed (black) and with the strong DIBs subtracted (blue), together with an approximate Gaussian fit to the broad emission component (red). While the fit is not perfect, it indicates that the asymmetry of the observed broad wings is essentially caused by the longward DIBs. These data are from the Galactic O-Star Spectroscopic Survey (GOSSS; Maíz Apellániz et al. 2011); they have a resolving power of 2500 obtained at the Gran Telescopio Canarias and will be fully discussed in a subsequent publication.

the WC system. However, Breysacher et al. (1999) quote a v magnitude of 11.75 for the "WC star," which clearly corresponds primarily to the B supergiant instead. The same remark applies to the magnitudes listed by SIMBAD, except for U. In contrast, the issue was correctly resolved by Prevot-Burnichon et al. (1981). In any event, this association should eventually yield valuable mutual clues to the basic parameters of both evolved objects. The VFTS 002/003 system is located at the edge of the survey field, far SW of the Tarantula Nebula, and is thus not directly associated with it (Figure 1).

The Hβ profile (Figure 3) shows the classic "Prussian Helmet" morphology, with a narrow P Cygni profile superimposed on the broad emission wings. Since this star is not near strong H II emission, a significant nebular contribution is not expected.

The spectral type of B1 Ia$^+$p is the earliest among the present sample; it is based upon the Si IV/Si III and Si III/He I absorption-line ratios (Figure 2) for the temperature and luminosity classes, respectively, allowing for LMC metal deficiency in the latter (Fitzpatrick 1991). The "p" is due to the Hβ profile. The N II spectrum is very strong, morphologically normal for the spectral type, which is expected to correspond to a significant physical enhancement. Indeed, McEvoy et al. (2015) have derived log(N/H)+12 (hereafter N/H) = 8.0 for VFTS 003; for comparison, Kurt & Dufour (1998) give an LMC baseline N/H of 6.9 determined from H II regions.

3.2. VFTS 533 = R142

The Hβ profile again appears to show the classic "Prussian Helmet" morphology, although in this case there is a substantial, blended nebular contribution to the narrow emission. Unlike in VFTS 003, the narrow Hα structure is very similar to that of Hβ. For reference in the context of the DIBs, $E_{B-V} = 0.49$.

The spectral type is B1.5 Ia$^+$p Nwk. Remarkably for a very high-luminosity object possibly nearing the LBV phase, the nitrogen lines are weaker than those of oxygen and carbon; while the N II lines are well marked, they are too weak for the spectral type, and the O II spectrum is much stronger. Compared with VFTS 003 discussed above, the slightly later type of VFTS 533 places it nearer to the normal N II maximum at B2, exacerbating the discrepancy. Fitzpatrick (1991) found the same anomalous nitrogen deficiency in the LMC B1–2 hypergiants Sanduleak (1970, Sk) −67°2, −68°26, and −69°221, as well as in several slightly less luminous supergiants. Another striking comparison of N-weak and N-strong objects at this type from the VFTS sample is shown by Evans et al. (2015, their Figure 1). McEvoy et al. (2015) have derived N/H of 7.4 for VFTS 533, consistent with the morphological appearance of the spectrum. With respect to the LMC baseline abundance cited above, the VFTS 533 value is certainly enhanced, but far less than that of other hyper/supergiants, e.g., VFTS 003.

Parker (1993) derived a spectral type of B0 Ia, and Walborn & Blades (1997; data from 1982) B0.5-B0.7 I; while the quality of the present data is far superior, nevertheless both of those classifications imply Si IV line strengths much greater than seen here. Thus a real spectral variation during an interval of 26 years appears likely. Moreover, the depth of the absorption component in the narrow P Cyg profile at Hβ increased by a factor of two to 20% of the continuum between VFTS epochs of 2008 October and December. During the same interval the metallic lines underwent a radial-velocity decrease of 12 km s^{-1} and a small intensity decrease, perhaps consistent with atmospheric motions as in the Galactic supergiant Sher 25 (Taylor et al. 2014).

As shown in Figure 1, this star is located just N(E) of R136 at the center of the nebula. However, it lies among the older stars identified as a separate cluster by Sabbi et al. (2012). Indeed, this spectral type is unlikely to be associated with the 1–2 Myr old, extremely early O and supermassive WNh stars in R136 (Crowther et al. 2010; P. A. Crowther et al. 2015, in preparation) Nevertheless, it is an extremely luminous star: with $M_V \sim -8$, it is one magnitude brighter than the typical Ia (Walborn 1972). With the bolometric corrections listed by Walborn et al. (2008, Table 2), the corresponding $M_{\rm bol}$ is -10.

3.3. VFTS 424 = R138

In this case, the narrow Hβ emission appears to be nebular, centered within a stellar absorption feature that in turn reverses the broad emission. It is probably not a coincidence that the spectral type is much later than those of VFTS 003 and 533, i.e., B9.5 Ia$^+$p with very strong Si II, Mg II, and Fe II absorption lines. The presence of N II λ3995 at such a late-type, albeit weak, may indicate an overabundance. The Hα emission profile is also a stellar/nebular composite; in this case $E_{B-V} = 0.33$.

VFTS 424 is also very near R136, although on the opposite (N)W side from VFTS 533. Still, it is most likely associated with the older population related to the Sabbi et al. (2012) cluster; see also Walborn & Blades (1997) and Selman et al. (1999) for more on the distribution of this population. VFTS 424 is also highly luminous, again with $M_V \sim -8$, albeit with $M_{\rm bol}$ only -8.4 because of the lower temperature.

3.4. VFTS 458 = P662

This star was suggested as an LBV candidate by Walborn & Blades (1997), albeit for different reasons; their data did not cover Hβ. Although the signal-to-noise ratio (S/N) was low, N II λ3995 appeared to be present with a strength greater than that of the adjacent He I λ4009, an anomaly for the spectral type of B6 Ia$^+$p. There also appeared to be a broad absorption consistent with an Fe II complex at 4550–4650 Å. Ironically, neither of those features has the same appearance in the superior VFTS data (Figure 2), although λ3995 and other N II lines are still too strong for the spectral type. The apparent broad feature is resolved into N II and Fe II lines in the VFTS data. McEvoy et al. derive N/H = 8.0. The triple Hβ structure is very similar to that of VFTS 424 and likely has similar origins. The Hα emission is again a stellar/nebular composite, and $E_{B-V} = 0.68$ is the largest in this sample consistent with the strongest λ6533 DIB.

VFTS 458 = Parker (1993) 662 is located about 2′ (30 pc in projection) south of R136, near the previously known LBV R143 and within the "R143 Association" first distinguished and discussed by Walborn & Blades (1997). It also has $M_V \sim -8$ (as does R143 itself in its current state), and $M_{\rm bol}$ of -8.6.

3.5. VFTS 739 = Sk −69°250

The Hβ profile of this star consists of only two components: the very broad emission wings and an approximately central stellar absorption reversal (Figure 3). Note that the lack of a central emission feature definitely eliminates electron scattering as the origin of the broad wings in this profile (cf. Hutsemékers & van Drom 1991). Remarkably, its Hα profile displays a second set of stronger, Be-like emission wings with a peak-to-peak separation of only 3.3 Å or 150 km s^{-1}. Such a profile in a supergiant does not necessarily imply the presence of a disk, as it can be produced by NLTE radiative transfer effects, as can the broad wings (Hubeny & Leitherer 1989; Puls et al. 1998). As further discussed in the next paragraph, this star is far from any nebulosity, thus supporting the interpretation of the profiles in the previous two spectra. The spectral type of A0 Iap is the latest of the five objects discussed here, while $E_{B-V} = 0.30$.

VFTS 739 does not belong to 30 Dor per se but is located even further to the south, at the northern edge of a large region of other discrete OB associations and scattered "field" stars. The comparably bright star to its immediate SE in Figure 1 is VFTS 764 = Sk −69°252 of type O9.7 Ia Nstr (Walborn et al. 2014), also indicative of a fairly advanced evolutionary stage. McEvoy et al. derive N/H = 7.8 for VFTS 764. The M_V of VFTS 739 is -7.2 ($M_{\rm bol} - 7.3$), while that of VFTS 764 is -7.4 ($M_{\rm bol} - 10.2$).

4. DISCUSSION

In addition to spectroscopic characteristics, photometric histories and circumstellar nebulae may provide information about the status of candidate or precursor LBVs. Here we briefly describe the results of some inquiries in those areas. Some Galactic counterparts to these VFTS objects and LBVs with similar Balmer profiles are also listed.

4.1. Photometric Variability

We investigated our targets in the ASAS and the OGLE shallow databases. The ASAS V data show apparent variability of VFTS 458 at the 1 mag level and of VFTS 739 at 0.3 mag. However, we are concerned about the bright nebulosity associated with the former (next subsection) and the latter range is near the accuracy limit. Indeed, the more precise OGLE data exclude variations at those levels for both stars; V and I data for VFTS 003, 424, 458, and 739 between HJD 2,453,000 and 2,455,000 show only a few points deviating by the order of 0.1 mag. (VFTS 533 was not reported.) Thus, we do not find LBV-like variability in light among the available data for these stars.

4.2. Circumstellar Nebulae

It is well known that the relatively rare giant eruptions of LBVs (as opposed to their more modest "outbursts" or photospheric expansions) eject nitrogen- and sometimes dust-rich circumstellar nebulae that may persist for thousands of years (Weis 2003; Walborn et al. 2008 and references therein). Hence, any such nebulae associated with our objects would be relevant to their evolutionary status.

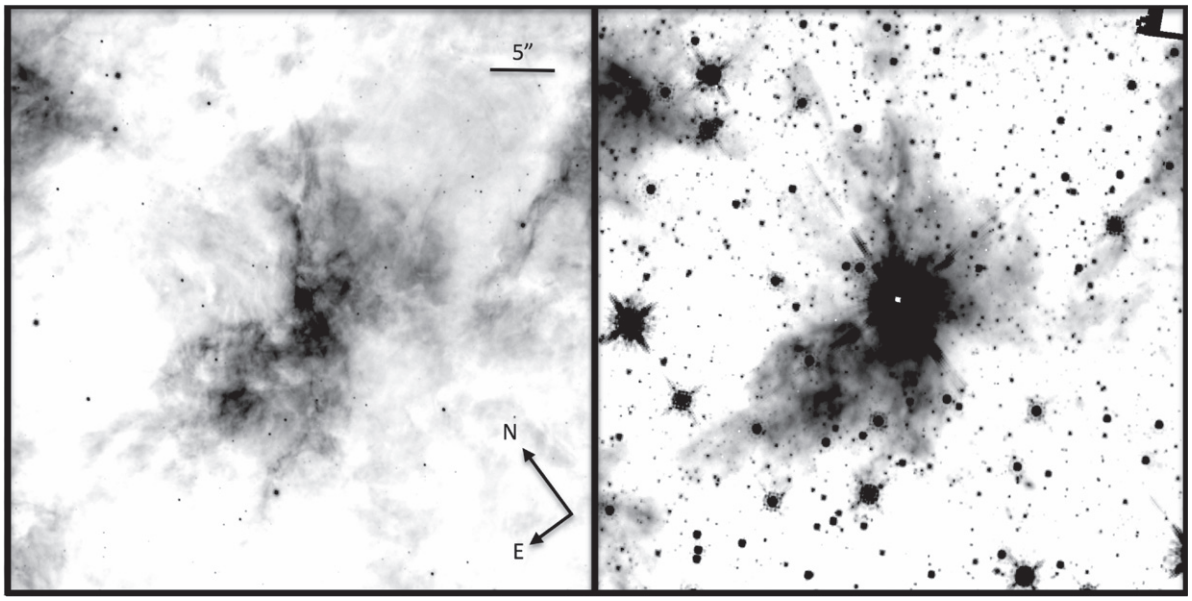

Figure 5. *HST* ACS Hα+[N II] (left) and WFC3 *H*-band (right) images of VFTS 458 (centered) and surrounding nebulosity. The brightest nebulosity has a roughly bipolar shape with numerous bright and dark condensations, suggestive of ejecta. The most prominent structures are similar between the two bands. (Note vestiges of the stellar diffraction spikes in the cardinal directions of the *H*-band image.) However, there is similarly structured nebulosity outside the frames to the W and E, so further data are required to establish the nature of the apparently associated nebulosity.

Accordingly, we have investigated available images from the *Hubble Space Telescope* cameras.

Sabbi et al. (2013) have described a massive Treasury Program in 30 Doradus using the Wide Field Camera 3 (WFC3) and Advanced Camera for Surveys (ACS) cameras, including NIR observations with the former and Hα with the latter. The Hα bandpass is 72 Å, which includes the adjacent [N II] lines. The optical image clearly shows the structured, asymmetrical ejected nebulosity associated with R143, discovered by Smith et al. (1998) and further discussed by Weis (2003).

The only one of our objects with a possibly associated nebulosity is VFTS 458, which appears centered in a relatively isolated, complex, asymmetrical (bipolar?) structure in both the optical and *H*-band images (Figure 5). We have further investigated this structure with two new optical spectroscopic datasets: three longslit position angles from the LCO 2.5 m Boller & Chivens cassegrain spectrograph ($R \sim 3000$) passing through the star and bright nebular knots; and three pointings with the ESO La Silla 2.2 m FEROS echelle spectrograph ($R = 48{,}000$) both on the star and a few arcseconds N or S of it. The principal result is even more extreme complexity of the region, with multiple nebular line components varying in both velocity and relative intensity on arcsecond scales, which these data are inadequate to fully characterize; further observations (preferably with IFUs) will be required to do so. Most importantly, we have not encountered any point with an [N II] λ6584/Hα intensity ratio greater than 10%, while ratios in the range 0.5–1 are typical of LBV and related circumstellar nebulae (references in the previous paragraph). Of course, the R143 nebula provides a cautionary note: most of the nebulosity projected near the star is ambient H II, but there are also compact knots of ejected processed material present. We note that the *Spitzer*/SAGE project (Meixner et al. 2006) found very bright [24] magnitudes of 2.4–2.8 for VFTS 458;[11] however, in view of the 6″ point-spread function (PSF) at 24 μm, further investigation is required to determine the exact source.

[11] http://irsa.ipac.caltech.edu/workspace/TMP_irnGZA_20171/Gator/irsa/23796/tbview.html

4.3. Galactic Counterparts

Several Galactic hypergiants or supergiants with the same peculiar Hβ profiles found in these LMC objects are known. To promote future comparative analyses, some details are provided here for several published cases. We are also aware of a number of unpublished ones that will appear in due course.

HD 190603, B1.5 Ia$^+$, has a Prussian Helmet profile, while HD 4841, B5 Ia, has the broad, asymmetrical wings with no central emission (Lennon et al. 1992, Figures 8 and 16, respectively). This atlas also displays many spectra throughout the B Ia sequence without such Hβ profiles.

ζ^1 Scorpii (HD 152236), B1.5 Ia$^+$, has a Prussian Helmet as well, which may be variable (Clark et al. 2012, Figure A.1). This spectrum is very similar to that of VFTS 533, albeit with much stronger nitrogen.

HD 80077, B2 Ia$^+$, also has a Prussian Helmet (Marco & Negueruela 2009, Figure 14). See also van Genderen (2001).

Cygnus OB2–12, B4 Ia$^+$, as classified here from the Si III/Si II ratio in the high-S/N GOSSS spectrogram shown in Figure 4, which shows its marked Prussian Helmet Hβ profile (see also Clark et al. 2012 again showing possible variability).

4.4. Anomalous Hβ Profiles in LBVs

Here we list several Luminous Blue Variables with references demonstrating the presence of Hβ profiles similar to those in the VFTS objects discussed. It should be recalled that the intensities of these broad wings are only a few percent above the continuum, so high S/N is required to detect them, as well as adequate intensity and wavelength scales to display them. They may be lost in some published LBV spectrograms, especially the extensive early photographic material.

HR Carinae (HD 90177) is the poster child for this phenomenon in LBVs, because of both its prominence and

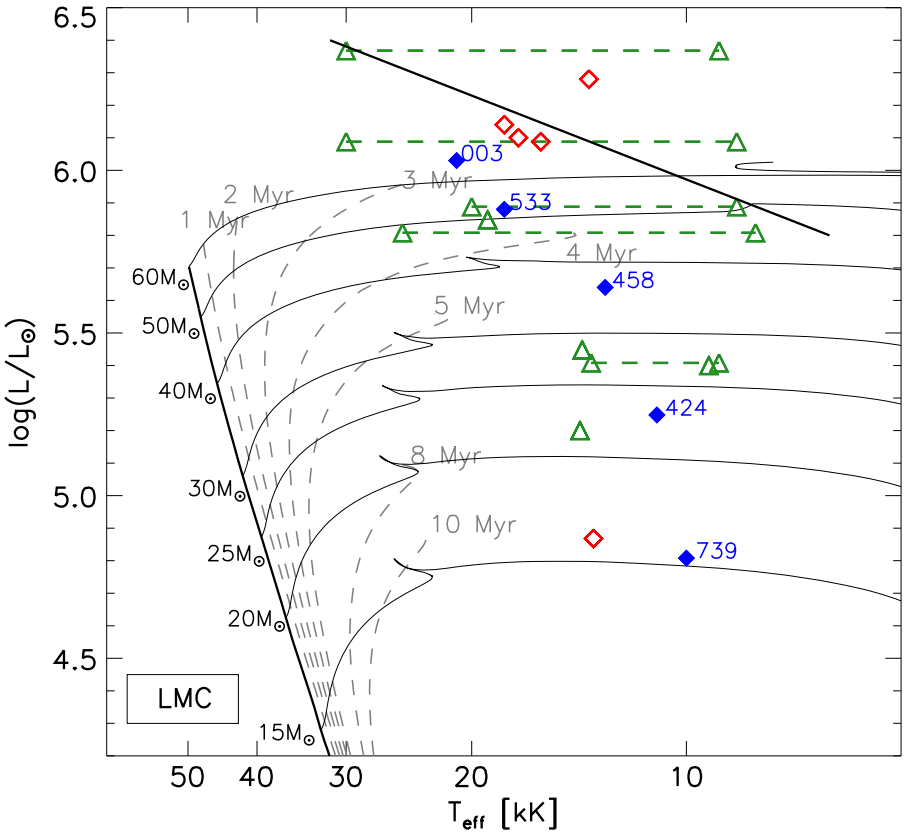

Figure 6. HRD comparing the locations of our VFTS objects (labeled blue diamonds; McEvoy et al. 2015; this paper) to those of Galactic hyper/supergiants (red diamonds—top to bottom Cyg OB2–12, HD 190603, ζ^1 Sco, HD 80077, HD 4841; Lennon et al. 1992; Marco & Negueruela 2009; Mel'nik & Dambis 2009; Clark et al. 2012) and LBVs or candidates (green triangles—top to bottom AG Car, R127, R143, P Cyg, S Dor, HR Car, R71, HD 168607, HD 168625; Humphreys & Davidson (HD) 1994; van Genderen 2001). The diagonal line at upper right is the HD Limit. The LMC evolutionary models are from Brott et al. (2011).

the fact that the discussion by Hutsemékers & van Drom (1991) is the only previous one addressing it to our knowledge. They show the asymmetrical Hβ profiles at both minimum and maximum phases of the LBV variation (their Figure 2). It can also be seen at minimum in Figure 8 of Walborn & Fitzpatrick (2000). Although at the limit of the data quality, that figure likely also shows the same asymmetrical Hβ wings in the neighboring LBV candidates HD 168607 and 168625, sans any central emission or P Cyg profile in the latter.

AG Carinae (HD 94910) likely also has this kind of Hβ profile at maximum in Figure 1 of Hutsemékers & Kohoutek (1988), although near the limit of the data and display.

R127 (HDE 269858) in the LMC shows the same asymmetrical Hβ wings upon entering its current extended outburst in Figure 3 of Stahl et al. (1983).

5. SUMMARY

We have discussed peculiar Hβ profiles in the spectra of five luminous hypergiants or supergiants in the 30 Doradus region, found in data from the VFTS. These profiles contain extremely broad wings (total width $\sim$3000 km s^{-1}), which are markedly asymmetrical, with a more extended, shallow slope shortward and a less extended, steeper slope longward. At the earlier B types a narrow, central P Cygni feature is also present (Prussian Helmet profile), whereas at mid-B to A types only the broad wings are seen. Identical profiles have been known for some time in a number of Galactic hypergiants. These Hβ profiles are quite different from those of Hα in the same spectra, which have more symmetrical emission wings except for a broad absorption depression in the shortward one.

Most importantly, we have proposed explanations of these peculiar, discrepant Balmer profiles in terms of broad Diffuse Interstellar Bands curtailing the longward wing of Hβ and depressing the shortward one of Hα.

Further, we have drawn attention to similar Hβ profiles in a number of both active and quiescent Luminous Blue Variables or candidates thereto. In Figure 6, the locations in a theoretical Hertzsprung-Russell Diagram of several hypergiants/supergiants with such profiles, including those discussed here, are shown in comparison with some LBVs. Note that the objects below the Humphreys–Davidson (HD) Limit may be returning from the red supergiant region. It is reasonable to hypothesize that the hyper/supergiants may be approaching the LBV state for the first time, which would be of considerable interest to the understanding of late massive stellar evolution if substantiated by further investigation. In fact, Cyg OB2–12 lies beyond the HD Limit on the assumption of association membership, which may be consistent with the presence of very massive O stars (Wright et al. 2015 and references therein). We note that our VFTS and related Galactic objects are unlikely to already be quiescent or post-LBVs, because established members of those categories have additional spectral peculiarities such as Fe II and [Fe II] emission lines, whereas the only peculiarities in these spectra are the broad Balmer wings.

We thank our colleagues Paul Crowther, Alex de Koter, Danny Lennon, Fabian Schneider, Nathan Smith, and Jorick

Vink, as well as an anonymous referee, for valuable discussions that contributed to this presentation. The SIMBAD database was useful to this research. R.H.B. acknowledges support from FONDECYT (Chile) via Regular Grant No. 1140076. J.M.A. acknowledges support from the Spanish Government Ministerio de Economía y competitividad (MINECO) through grant AYA2013-40\,611-P. Publication support was provided by the STScI Director's Discretionary Research Fund. The Space Telescope Science Institute is operated by AURA, Inc., under NASA contract NAS5-26555.

REFERENCES

Bernat, A. P., & Lambert, D. L. 1978, PASP, 90, 520
Breysacher, J., Azzopardi, M., & Testor, G. 1999, A&AS, 137, 117
Brott, I., de Mink, S. E., Cantiello, M., et al. 2011, A&A, 530, A115
Clark, J. S., Najarro, F., Negueruela, I., et al. 2012, A&A, 541, A145
Crowther, P. A., Lennon, D. J., & Walborn, N. R. 2006, A&A, 446, 279
Crowther, P. A., Schnurr, O., Hirschi, R., et al. 2010, MNRAS, 408, 731
Evans, C. J., Kennedy, M. B., Dufton, P. L., et al. 2015, A&A, 574, A13
Evans, C. J., Taylor, W. D., Hénault-Brunet, V., et al. 2011, A&A, 530, A108
Feast, M. W., Thackeray, A. D., & Wesselink, A. J. 1960, MNRAS, 121, 337
Fitzpatrick, E. L. 1991, PASP, 103, 1123
Herbig, G. H. 1995, ARA&A, 33, 19
Hubeny, I., & Leitherer, C. 1989, PASP, 101, 114
Humphreys, R. M., & Davidson, K. 1994, PASP, 106, 1025
Hutsemékers, D., & Kohoutek, L. 1988, A&AS, 73, 217
Hutsemékers, D., & van Drom, E. 1991, A&A, 248, 141
Kurt, C. M., & Dufour, R. J. 1998, RMxAC, 7, 202
Lennon, D. J., Dufton, P. L., & Fitzsimmons, A. 1992, A&AS, 94, 569
Maíz Apellániz, J. 2013, in Proc. of the X Scientific Meeting of the Spanish Astronomical Society (SEA), Highlights of Spanish Astrophysics VII, ed. J. C. Guirado, L. M. Lara, V. Quilis, & J. Gorgas, 583
Maíz Apellániz, J., Sota, A., Barbá, R. H., et al. 2014, IAU Symp. 297, The Diffuse Interstellar Bands (Paris: IAU), 117
Maíz Apellániz, J., Sota, A., Walborn, N. R., et al. 2011, in Proc. of the IX Scientific Meeting of the Spanish Astronomical Society (SEA), Highlights of Spanish Astrophysics VI, ed. M. R. Zapatero Osorio, J. Gorgas, J. Maiz Apellániz, J. R. Pardo, & A. Gil de Paz, 467
Marco, A., & Negueruela, I. 2009, A&A, 493, 79
McEvoy, C. M., Dufton, P. L., Evans, C. J., et al. 2015, A&A, 575, A70
Meixner, M., Gordon, K. D., Indebetouw, R., et al. 2006, AJ, 132, 2268
Mel'nik, A. M., & Dambis, A. K. 2009, MNRAS, 400, 518
Najarro, F. (P.), & Hillier, D. J. 2012, ASSL, 384, 67
Parker, J. Wm. 1993, AJ, 106, 560
Parker, J. Wm., Clayton, G. C., Winge, C., et al. 1993, ApJ, 409, 770
Pasquini, L., Avila, G., Blecha, A., et al. 2002, ESO Messenger, 110, 1
Prevot-Burnichon, M. L., Prevot, L., Rebeirot, E., et al. 1981, A&A, 103, 83
Puls, J., Kudritzki, R.-P., Santolaya-Rey, A. E., et al. 1998, ASPC, 131, 245
Sabbi, E., Anderson, J., Lennon, D. J., et al. 2013, AJ, 146, 53
Sabbi, E., Lennon, D. J., Gieles, M., et al. 2012, ApJL, 754, L37
Sana, H., de Koter, A., de Mink, S. E., et al. 2013, A&A, 550, A107
Sanduleak, N. 1970, CTIO Contribution, No. 89
Santolaya-Rey, A. E., Puls, J., & Herrero, A. 1997, A&A, 323, 488
Selman, F., Melnick, J., Bosch, G., et al. 1999, A&A, 347, 532
Smith, L. J., Nota, A., Pasquali, A., et al. 1998, ApJ, 503, 278
Stahl, O., Wolf, B., Klare, G., et al. 1983, A&A, 127, 49
Stahl, O., Wolf, B., Leitherer, C., et al. 1985, A&AS, 61, 237
Taylor, W. D., Evans, C. J., Simón-Díaz, S., et al. 2014, MNRAS, 442, 1483
van Genderen, A. M. 2001, A&A, 366, 508
Walborn, N. R. 1972, AJ, 77, 312
Walborn, N. R. 1997, ASPC, 120, 8
Walborn, N. R., & Blades, J. C. 1997, ApJS, 112, 457
Walborn, N. R., & Fitzpatrick, E. L. 2000, PASP, 112, 50
Walborn, N. R., & Howarth, I. D. 2000, PASP, 112, 1446
Walborn, N. R., Sana, H., Simón-Díaz, S., et al. 2014, A&A, 564, A40
Walborn, N. R., Stahl, O., Gamen, R. C., et al. 2008, ApJL, 683, L33
Weis, K. 2003, A&A, 408, 205
Wright, N. J., Drew, J. E., & Mohr-Smith, M. 2015, MNRAS, 449, 741